Supporting Information

A Multi-Scale Approach to the Dissociative Adsorption of Oxygen on Highly-Dispersed Platinum Supported on γ-Al_2O_3

Alexis Sangnier,[1] Mickaël Matrat,[1] André Nicolle,[1] Christophe Dujardin,[2] Céline Chizallet[3,]*

[1]Powertrain and Vehicle Division, IFP Energies Nouvelles – 1 et 4 avenue de Bois-Préau – 92852 Rueil-Malmaison Cedex, (France) ; Institut Carnot IFPEN Transports Energies

[2]Univ. Lille, ENSCL, Centrale Lille, CNRS, Univ. Artois, UCCS UMR 8181, 59000 Lille, (France)

[3]IFP Energies Nouvelles – Rond-Point de l'Echangeur de Solaize – BP 3, 69360 Solaize, (France)

Corresponding author: celine.chizallet@ifpen.fr

S1. Illustration of a typical velocity-scaled MD run with cluster reconstruction

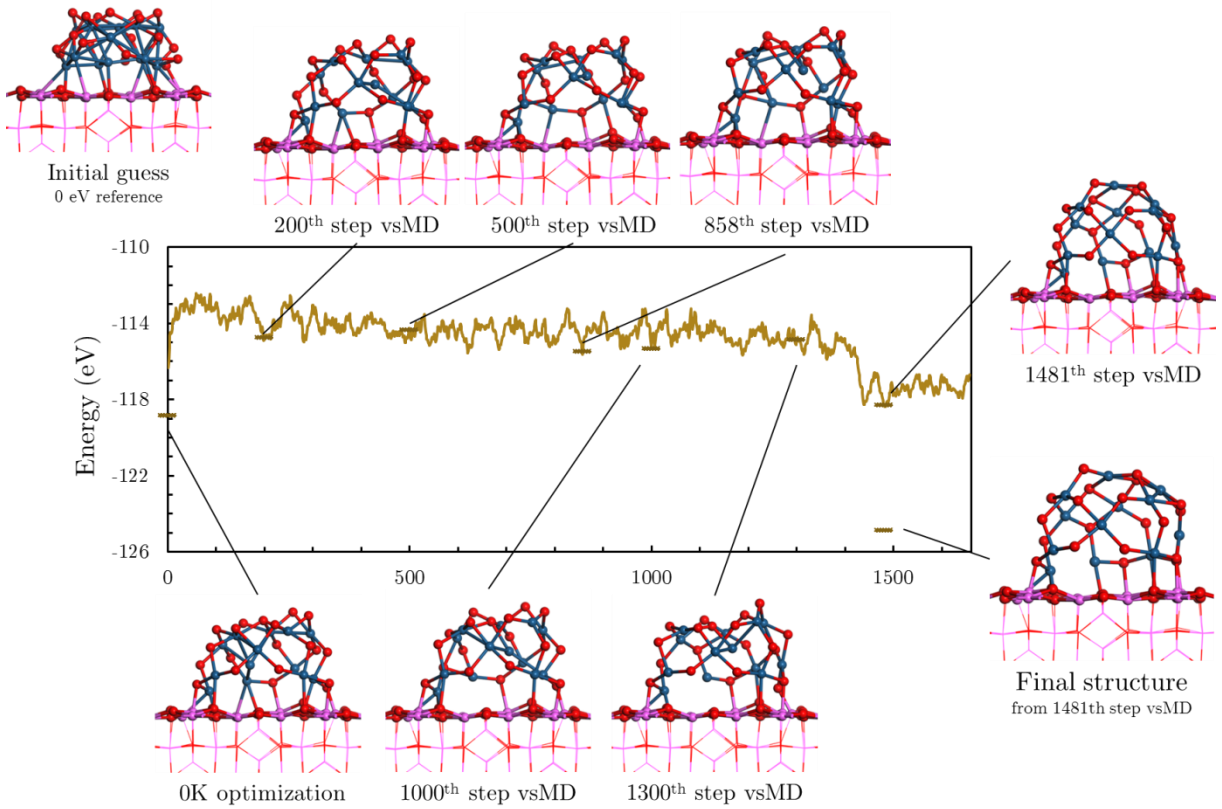

Figure S1. Energies and illustrations of $Pt_{13}O_{20}$ structure through the optimization process: optimization – velocity-scaled molecular dynamics at 600K and 5fs. The initial (0K) and final structures were obtained by geometry optimization (quench for the final structure). Aluminum: purple, oxygen: red, platinum: blue.

S2. Estimation of the Gibbs free energy of adsorption

Gibbs free energy was calculated with the following equations, with E the electronic energy, S the entropies, U internal energies, P the pressure and V_m the molar volume.

$$G(T,p) = E + U_{trans}(T,p) + U_{vib}(T,P) + U_{rot}(T,p) + PV_m - T(S_{trans}(T,p) + S_{vib}(T,p) + S_{rot}(T,p)) \quad \text{(Equation S1)}$$

$$U_{vib}(T) = N_A \left[\sum_n \frac{1}{2} h\nu_n + \sum_n \frac{hc\nu_n \times \exp\left(-\frac{h\nu_n}{k_B T}\right)}{1-\exp\left(-\frac{h\nu_n}{k_B T}\right)} \right] \quad \text{(Equation S2)}$$

For the gas specie O_2, equation S3 is used. In the case of condensed systems ($Pt_{13}O_n/\gamma\text{-}Al_2O_3$), these terms are considered to be zero, as well as rotational and translational entropies given by equations (S5) and (S6).

$$U_{trans}(T) + U_{rot}(T) + PV_m(T) = 7/2RT \quad \text{(Equation S3)}$$

$$S_{vib}(T) = N_A k_B \left[\sum_n \frac{\frac{hc\nu_n}{k_B T} \times \exp\left(-\frac{h\nu_n}{k_B T}\right)}{1-\exp\left(-\frac{h\nu_n}{k_B T}\right)} - \sum_n ln\left(1 - \exp\left(-\frac{h\nu_n}{k_B T}\right)\right) \right] \quad \text{(Equation S4)}$$

$$S_{rot}(T) = N_A k_B \left(\frac{3}{2} + ln\left[\frac{\sqrt{\pi}}{\sigma} \left(\frac{8\pi^2 k_B T}{h^2} \right)^{\frac{3}{2}} \sqrt{A_e \times B_e \times C_e} \right] \right) \quad \text{(Equation S5)}$$

$$S_{trans}(T,p) = N_A k_B \left(\frac{5}{2} + ln\left(\frac{RT}{P} \left(\frac{2\pi M \quad k_B T}{h^2} \right)^{3/2} \right) \right) \quad \text{(Equation S6)}$$

With ν_n the vibrational frequencies of the system (vibration eigenvalues), k_B the Boltzmann constant, N_A the Avogadro constant, T the temperature, h the Planck constant and M the molar weight. σ corresponds to the symmetry number of the system and A_e ,B_e and C_e the moments of inertia according to the eigenaxes of the molecule. The determination of the oxygen-adsorption free energy G used to build the thermodynamic diagrams is detailed in equation 2. The different domains of coverages present on the diagrams reflect the minimum free energy among other coverage systems.

S3. X-Ray fluorescence for the two catalysts

Table S1. X-Ray fluorescence results

Catalysts	X-Ray fluorescence	
	Pt (wt. %)	Cl (wt. %)
0.3 wt. % Pt/γ-Al_2O_3	0.30	0.08
1.0 wt. % Pt/γ-Al_2O_3	1.03	0.08

S4. Optimization of the TPD protocol

A first set of O_2-TPD experiments was performed on the 1 wt % Pt/γ-Al_2O_3 material to investigate the impact of the high temperatures reached in the TPD experiments. The sample underwent dehydrations at 300°C or 600°C before TPD. Water release was observed (Figure S2-a) on a large range of temperatures, always starting at the dehydration temperature up to the final one (1100°C). This phenomenon can be attributed to the dehydroxylation of the surface of gamma alumina.[1-5] Moreover, the expected oxygen release follows a similar trends than water release, with a H_2O/O_2 ratio of intensities around 100 to 1. This suggests a possible impact of water release on oxygen desorption in a way that is not elucidated. Thus it can perturb the interpretation of the O_2 desorption from the nanoparticles in the case of the supported catalysts. Hence we tried to minimize water release with appropriate dehydration conditions.

Figure S2-b illustrates the effect of the duration of the dehydration step on the water release during O_2-TPD for the 1 wt % Pt/γ-Al_2O_3 system. The signals related to water are similar after a dehydration of 300°C whatever the dehydration duration (1 or 5 h). Nevertheless there is a significant difference for 600°C dehydration experiments. The intensity of the peaks and their width are weaker after 5h dehydration rather than 1h dehydration. This is in line with the work of Lagauche et al.[2] showing that during a TPD most of the water is released before 600°C, but they still found few hydroxyl groups on the surface.

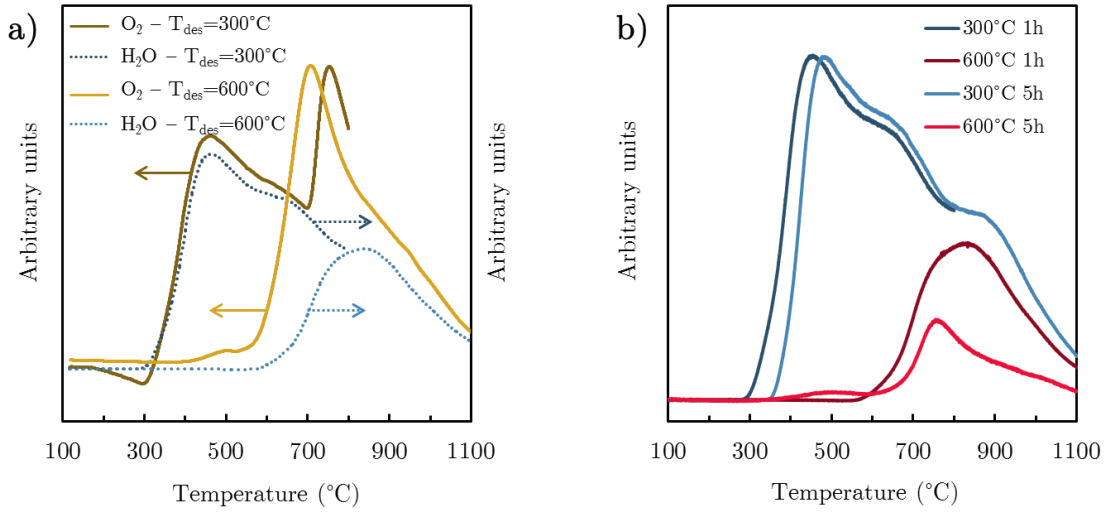

Figure S2. a) Relative signals of oxygen (m/z=32) and water (m/z=18) during the O_2-TPD 1 wt % Pt/Al_2O_3 with a dehydration temperatures of 300°C and 600°C for 1 hour prior to the TPD experiment. b) Relative signals of water (m/z=32) during TPD experiments on 1 wt % Pt/A_2O_3 according to different dehydration conditions.

In order to obtain a highly dehydrated material to limit the effect of water, a five hours dehydration step at 600°C was selected, prior to TPD (Figure S3). Moreover, the mass spectrometry signals of O_2 for alumina alone were deduced from that of the catalysts obtained with the same treatment conditions. Thus we avoid a possible contribution of O_2 adsorption on alumina.

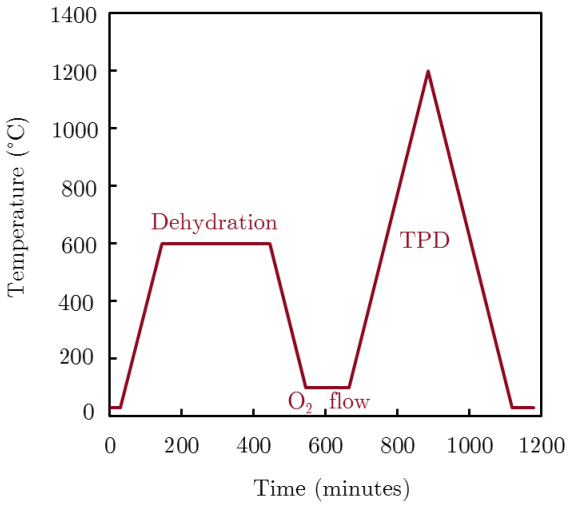

Figure S3. Definitive temperature process during TPD experiments

S5. Deconvolution of the TPD profiles

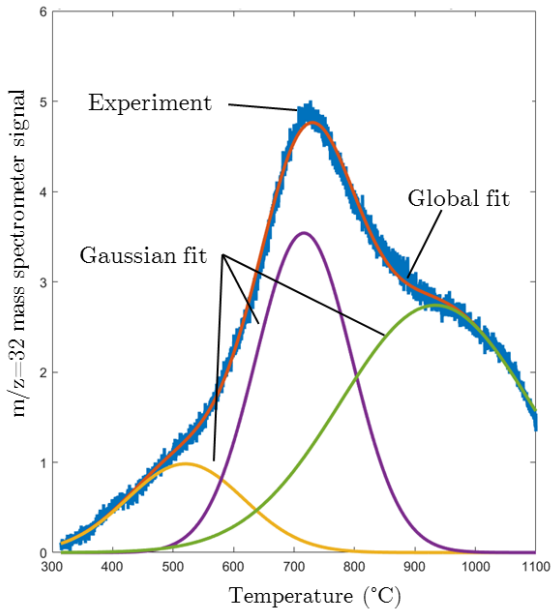

Figure S4. Deconvolution fit of the MS signal m/z=32 recorded during TPD for the 0.3wt % Pt/γ-Al_2O_3 catalyst using three Gaussian-type fitting curves. The global fit curve is the sum of the three Gaussian curves.

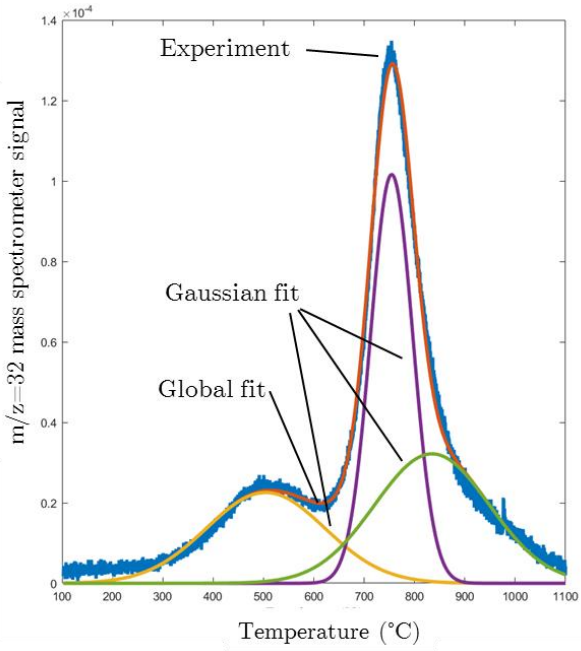

Figure S5. Deconvolution fit of the MS signal m/z=32 for the 1wt % Pt/γ-Al_2O_3 catalyst using three Gaussian-type fitting curves. The global fit curve is the sum of the three Gaussian curves.

S6. Dissociative adsorption of O_2 on Pt(111) investigated by ab initio calculations

Pt(111) was considered to account for bigger particles that may be formed during the TPD experiments. It also provides a good reference case. Atomic oxygen coverages from 0 to 1 monolayer were simulated (Figure S6). The well-known p(2x2) periodic surface patterns were calculated.[6-7] The oxygen atoms were found only in fcc hollow site, in agreement with the literature,[8-12] whatever the coverage. Our adsorption energies (table S2) are quite close to the ones of Pang et al.[12] who uses the same ab initio level of theory (GGA PBE). The comparison with older simulations is not easy as the functionals used are different.[8] Stepped surfaces[9,13] show a mildly higher oxygen stability and a slightly larger coverage capacity. These kind of structures are likely to undergo platinum surface reconstruction.[14]

For 0.75ML and 1ML coverages, subsurface oxygen atoms simulations were performed but found energetically unfavored. It is however known that adsorbed oxygen can lead to the formation of an oxide.[15-16] The investigation of such surface structure would require a dedicated study that is beyond the scope of the present work.

The mean adsorption energy (table S2) was found to get less favorable with increasing oxygen coverage. A thermodynamic diagram was also constructed to evaluate the difference with previous Pt(111) studies (Figure S7) and compare with Pt_{13} in a consistent way. As the adsorption are found more favorable than the one reported by Legaré,[8] the phase diagram induced coverages domain shifted to higher temperature. Our calculations are however close to the latest work of Pang et al.[12]

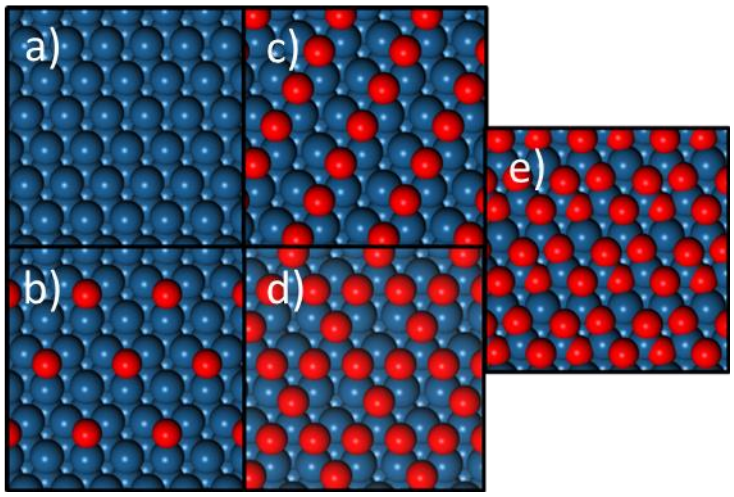

Figure S6. Illustrations of simulated Pt(111)-nO surfaces (top views) with no oxygen (a), 0.25ML (b), 0.5ML (c), 0.75ML (d) and 1ML (e). Platinum atoms are in blue, oxygen in red.

Table S2. Atomic heat of adsorption per O_2 found for Pt(111) systems according to equation 1.

Oxygen coverage (ML)	$E_{adsorption}$ (kcal.mol^{-1})
0.25	-81.3
0.50	-69.2
0.75	-53.5
1.0	-37.3

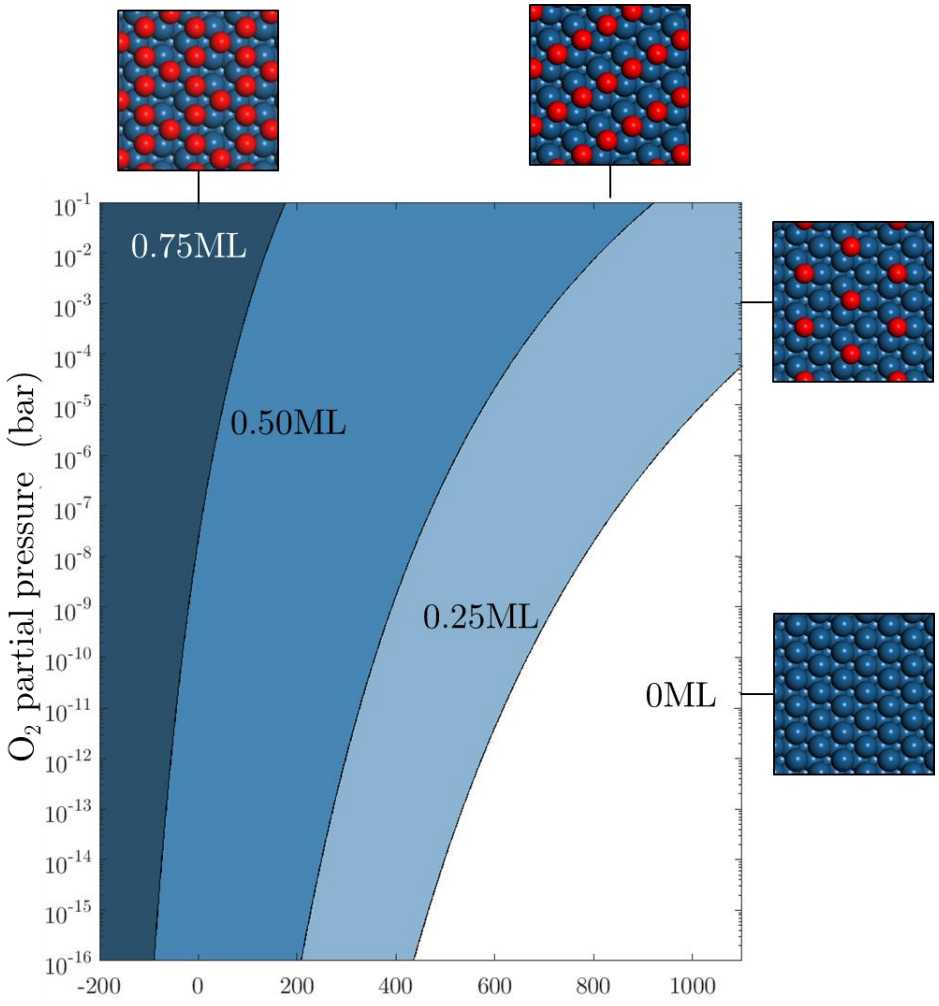

Figure S7. Thermodynamic diagram (p_{O2},T) for the adsorption of atomic O on Pt(111).

S7. Most stable structures found for the supported $Pt_{13}O_n$ system from ab initio calculations

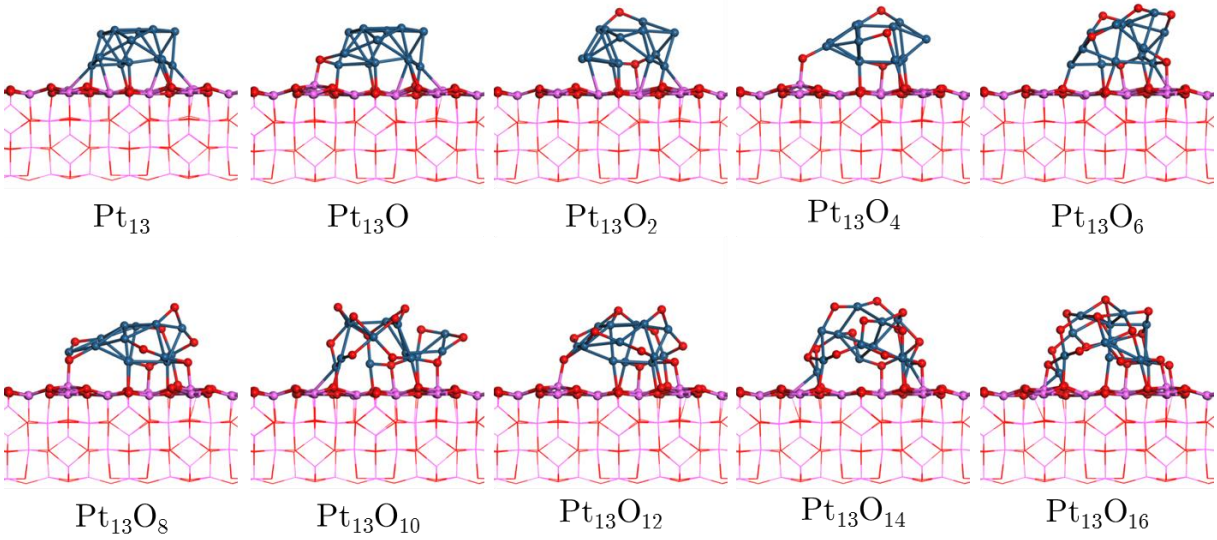

Figure S8. Illustrations of the two-layers $Pt_{13}O_n$ structures (side views).

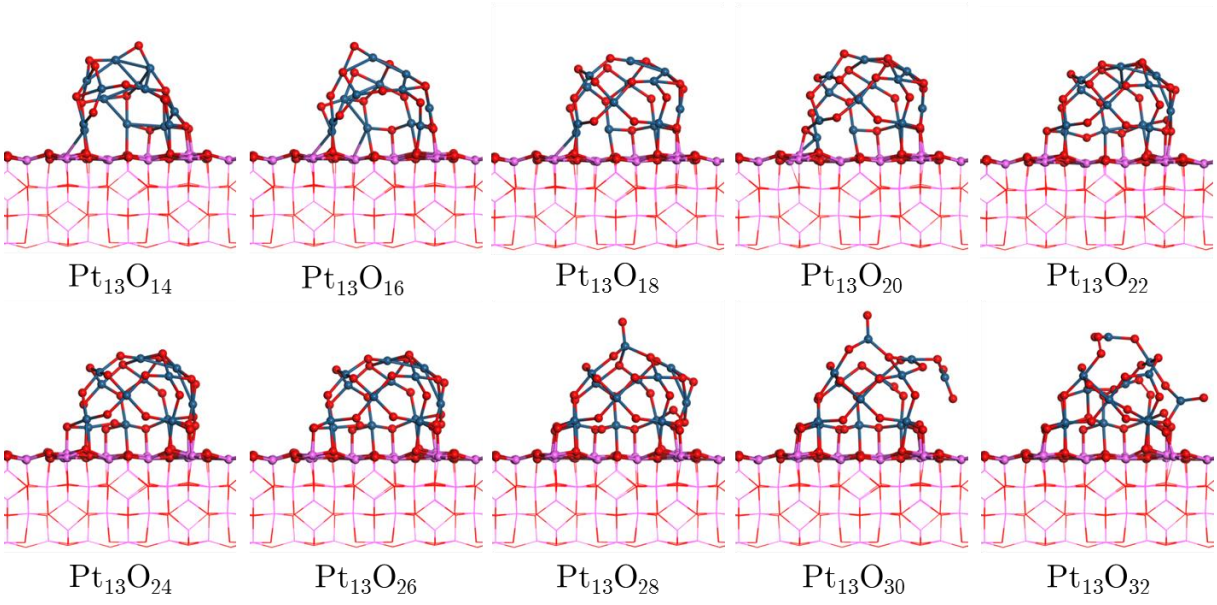

Figure S9. Illustrations of the hemispheric $Pt_{13}O_n$ structures (side views).

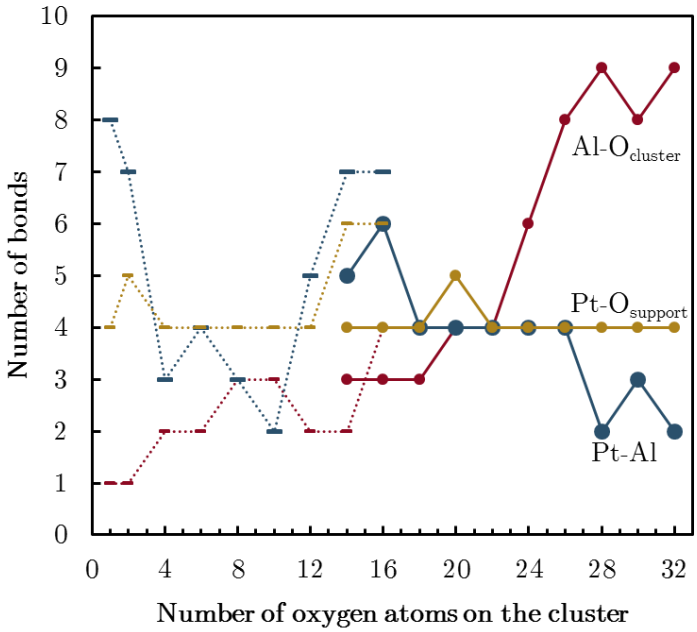

Figure S10. Number of bonds between the cluster and the support (Pt-Al, Al-$O_{cluster}$ and Pt-$O_{support}$). The maximum bond length for the count was 2.5 Å. Dotted lines corresponds to the two-layers structures whereas plain lines are hemispheric structures data.

S8. Transition structures for the dissociation of O_2

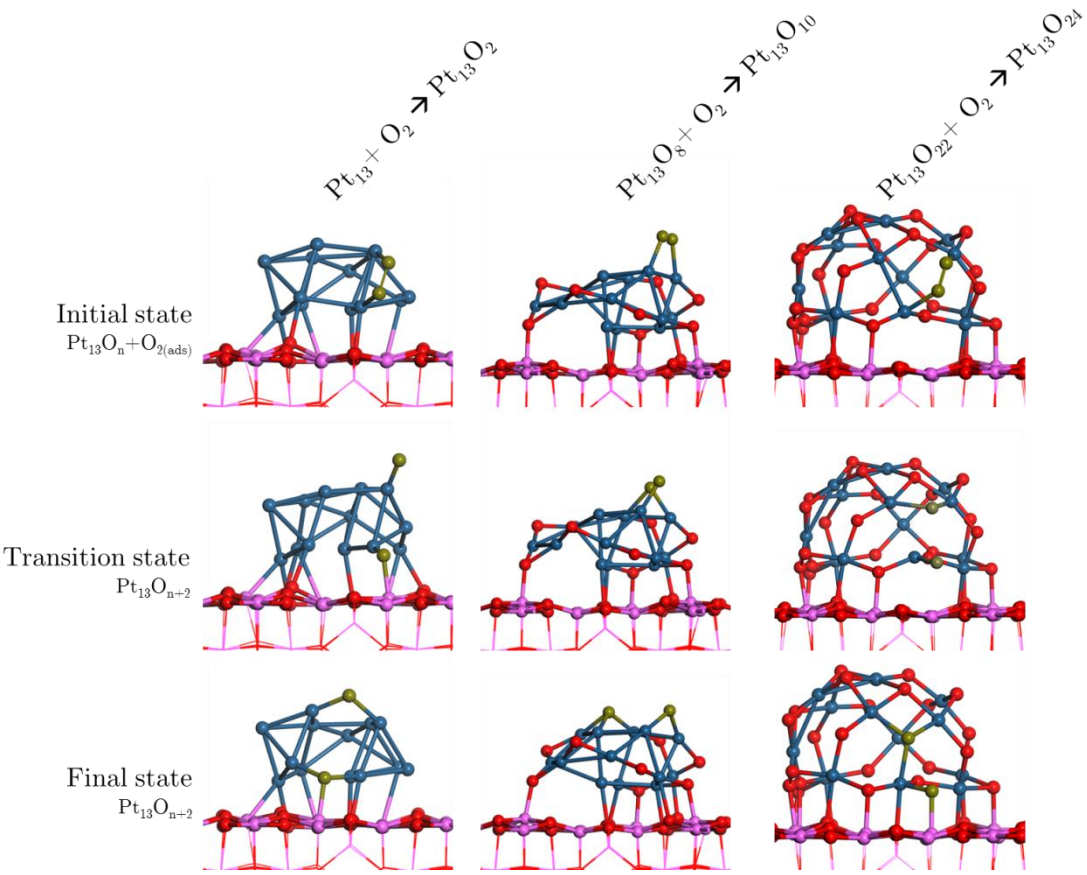

Figure S11. Configurations of initial, transition and final states for the three coverages investigated for dissociation of O_2 on $Pt_{13}O_n/\gamma\text{-}Al_2O_3$. The oxygen atoms engaged in dissociation are set in brown.

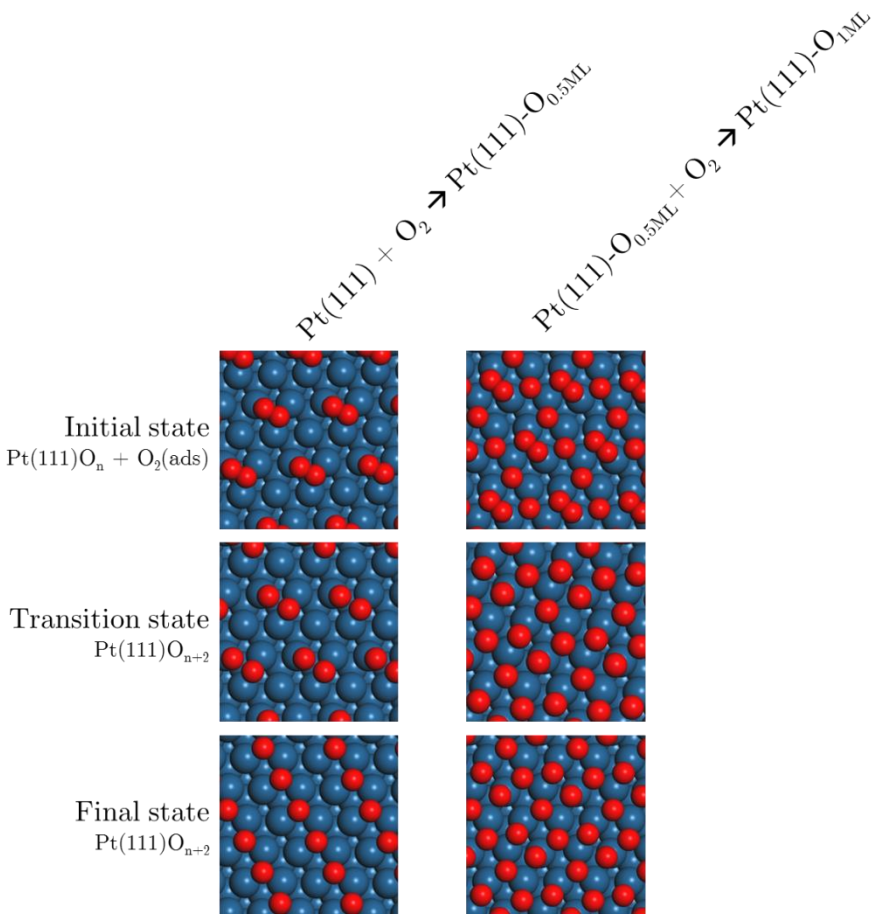

Figure S12. Configurations of initial, transitions and final states for the two coverages investigated for dissociation of O_2 on Pt(111).

Table S3. Transition state characteristics for $Pt_{13}O_n$ and Pt(111) structures.

Transition state	Imaginary frequency (cm^{-1})	O-O bond length (Å)
$Pt_{13}O_2$	32	4.26
$Pt_{13}O_{10}$	57	3.01
$Pt_{13}O_{24}$	118*	3.09
Pt(111)-0.5ML	256	1.91
Pt(111)-1ML	109	2.37

* For this system, the removal of two spurious additional imaginary frequencies (33 and 62 i cm^{-1}) appeared to be impossible, even by using more stringent convergence criteria. This does not affect the further kinetic modeling, the adsorption constant being parameterized thanks to a sticking coefficient.

S9. Kinetic parameters for the $Pt_{13}O_n$ model and Pt(111) model

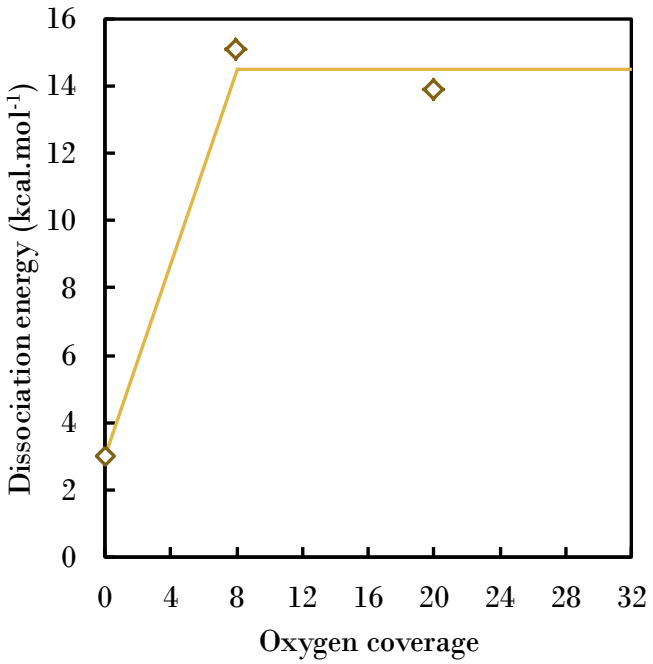

Figure S13. Dissociation activation energy for the supported Pt_{13} system. Diamonds are the DFT-determined values, lines are the piecewise linear trends chosen in the kinetic model.

Table S4. Reactions and kinetic parameters of the Pt(111) model with a sticking coefficient of 0.01

Reaction	Forward parameters			Backward parameters		
	Sticking coefficient	β	$E_{dissociation}$ (kcal.mol^{-1})	Pre-exponential factor (mol.s^{-1}.cm^{-2})	β	$E_{activation}$ (kcal.mol^{-1})
O_2 + 2 Pt ↔ 2 PtO	0.01	0	34.7	4.19E+29	0.5	119
O_2 + 2 PtO ↔ 2 PtO_2	0.01	0	85.3	4.19E+29	0.5	128
O_2 + 2 PtO_2 ↔ 2 PtO_3	0.01	0	136	8.72E+29	0.5	94.9
O_2 + 2 PtO_3 ↔ 2 PtO_4	0.01	0	186	1.04E+30	0.5	104

Table S5. Reactions and kinetic parameters of the $Pt_{13}O_n$ model with a sticking coefficient of 0.01

Adsorption reactions	Forward parameters			Backward parameters		
	Sticking coefficient	β	$E_{dissociation}$ (kcal.mol^{-1})	Pre-exponential factor (s^{-1})	β	$E_{activation}$ (kcal.mol^{-1})
$O_2 + Pt_{13} \leftrightarrow Pt_{13}O_2$	0.01	0	2.97	2.80E+18	0.5	119
$O_2 + Pt_{13}O_2 \leftrightarrow Pt_{13}O_4$	0.01	0	5.84	4.01E+18	0.5	128
$O_2 + Pt_{13}O_4 \leftrightarrow Pt_{13}O_6$	0.01	0	8.72	6.48E+18	0.5	94.9
$O_2 + Pt_{13}O_6 \leftrightarrow Pt_{13}O_8$	0.01	0	11.6	4.86E+18	0.5	104
$O_2 + Pt_{13}O_8 \leftrightarrow Pt_{13}O_{10}$	0.01	0	14.5	1.17E+17	0.5	96.5
$O_2 + Pt_{13}O_{10} \leftrightarrow Pt_{13}O_{12}$	0.01	0	14.5	4.20E+18	0.5	40.2
$O_2 + Pt_{13}O_{12} \leftrightarrow Pt_{13}O_{14}$-TL	0.01	0	14.5	2.27E+21	0.5	104
$O_2 + Pt_{13}O_{12} \leftrightarrow Pt_{13}O_{14}$-HM	0.01	0	14.5	2.28E+20	0.5	100
$O_2 + Pt_{13}O_{14}$-TL $\leftrightarrow Pt_{13}O_{16}$-TL	0.01	0	14.5	3.04E+19	0.5	126
$O_2 + Pt_{13}O_{14}$-HM $\leftrightarrow Pt_{13}O_{16}$-HM	0.01	0	14.5	1.02E+18	0.5	26.0
$O_2 + Pt_{13}O_{16}$-TL $\leftrightarrow Pt_{13}O_{18}$	0.01	0	14.5	2.40E+16	0.5	38.8
$O_2 + Pt_{13}O_{16}$-HM $\leftrightarrow Pt_{13}O_{18}$	0.01	0	14.5	7.13E+18	0.5	99.1
$O_2 + Pt_{13}O_{18} \leftrightarrow Pt_{13}O_{20}$	0.01	0	14.5	2.60E+23	0.5	120
$O_2 + Pt_{13}O_{20} \leftrightarrow Pt_{13}O_{22}$	0.01	0	14.5	1.86E+23	0.5	53.3
$O_2 + Pt_{13}O_{22} \leftrightarrow Pt_{13}O_{24}$	0.01	0	14.5	2.26E+23	0.5	43.7
$O_2 + Pt_{13}O_{24} \leftrightarrow Pt_{13}O_{26}$	0.01	0	14.5	3.41E+23	0.5	21.3
$O_2 + Pt_{13}O_{26} \leftrightarrow Pt_{13}O_{28}$	0.01	0	14.5	2.14E+23	0.5	24.8
$O_2 + Pt_{13}O_{28} \leftrightarrow Pt_{13}O_{30}$	0.01	0	14.5	1.26E+23	0.5	25.4
$O_2 + Pt_{13}O_{30} \leftrightarrow Pt_{13}O_{32}$	0.01	0	14.5	6.70E+23	0.5	31.7
Surface reactions	Pre-exponential factor (s^{-1})	β	$E_{activation}$ (kcal.mol^{-1})	Pre-exponential factor (s^{-1})	β	$E_{activation}$ (kcal.mol^{-1})
$Pt_{13}O_{14}$-TL $\leftrightarrow Pt_{13}O_{14}$-HM	1E+11	0.5	0	1E+11	0.5	11.0
$Pt_{13}O_{16}$-TL $\leftrightarrow Pt_{13}O_{16}$-HM	1E+11	0.5	74.6	1E+11	0.5	0

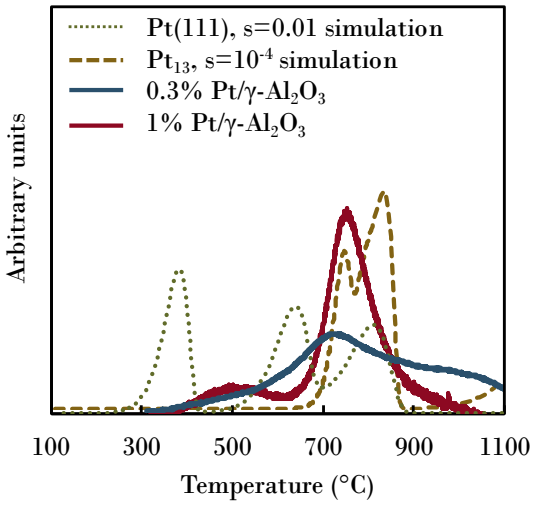

Figure S14. Predicted O_2 concentration profile during O_2-TPD with Pt(111) and Pt_{13}, with TPD experiments on highly-dispersed Pt/ γ -Al_2O_3. For Pt_{13}, the sticking coefficient is set to 10^{-4}.

References

(1) Digne, M.; Sautet, P.; Raybaud, P.; Euzen, P.; Toulhoat, H., Hydroxyl Groups on Gamma-Alumina Surfaces: a DFT Study, *J. Catal.* **2002**, *211*, 1-5.

(2) Lagauche, M.; Larmier, K.; Jolimaitre, E.; Barthelet, K.; Chizallet, C.; Favergeon, L.; Pijolat, M., Thermodynamic Characterization of the Hydroxyl Group on the γ-Alumina Surface by the Energy Distribution Function, *J. Phys. Chem. C* **2017**, *121*, 16770-16782.

(3) Ballinger, T. H.; Yates, J. T., IR Spectroscopic Detection of Lewis Acid Sites on Alumina Using Adsorbed Carbon Monoxide. Correlation with Aluminum-Hydroxyl Group Removal, *Langmuir* **1991**, *7*, 3041-3045.

(4) Liu, X., DRIFTS Study of Surface of γ-Alumina and Its Dehydroxylation, *J. Phys. Chem. C* **2008**, *112*, 5066-5073.

(5) Wischert, R.; Laurent, P.; Copéret, C.; Delbecq, F.; Sautet, P., γ-Alumina: The Essential and Unexpected Role of Water for the Structure, Stability, and Reactivity of "Defect" Sites, *J. Am. Chem. Soc.* **2012**, *134*, 14430-14449.

(6) Bleakley, K.; Hu, P., A Density Functional Theory Study of the Interaction between CO and O on a Pt Surface: CO/Pt(111), O/Pt(111), and CO/O/Pt(111), *J. Am. Chem. Soc.* **1999**, *121*, 7644-7652.

(7) Parker, D. H.; Bartram, M. E.; Koel, B. E., Study of High Coverages of Atomic Oxygen on the Pt(111) Surface, *Surf. Sci.* **1989**, *217*, 489-510.

(8) Légaré, P., Interaction of Oxygen with the Pt(111) Surface in Wide Conditions Range. A DFT-Based Thermodynamical Simulation, *Surf. Sci.* **2005**, *580*, 137-144.

(9) Bray, J. M.; Smith, J. L.; Schneider, W. F., Coverage-Dependent Adsorption at a Low Symmetry Surface: DFT and Statistical Analysis of Oxygen Chemistry on Kinked Pt(321), *Topics Catal.* **2013**, *57*, 89-105.

(10) Fu, Q.; Yang, J.; Luo, Y., A First Principles Study on the Dissociation and Rotation Processes of a Single O2Molecule on the Pt(111) Surface, *J. Phys. Chem. C* **2011**, *115*, 6864-6869.

(11) Watwe, R. M.; Cortright, R. D.; Mavrikakis, M.; Norskov, J. K.; Dumesic, J. A., Density Functional Theory Studies of the Adsorption of Ethylene and Oxygen on Pt(111) and Pt_3Sn(111), *J. Chem. Phys.* **2001**, *114*, 4663-4668.

(12) Pang, Q.; Zhang, Y.; Zhang, J.-M.; Xu, K.-W., Structural and Electronic Properties of Atomic Oxygen Adsorption on Pt(111): A Density-Functional Theory Study, *Appl. Surf. Sci.* **2011**, *257*, 3047-3054.

(13) Wang, J. G.; Li, W. X.; Borg, M.; Gustafson, J.; Mikkelsen, A.; Pedersen, T. M.; Lundgren, E.; Weissenrieder, J.; Klikovits, J.; Schmid, M.et al, One-Dimensional PtO_2 at Pt Steps: Formation and Reaction with CO, *Phys. Rev. Lett.* **2005**, *95*, 256102.

(14) Zhu, T.; Sun, S.-G.; van Santen, R. A.; Hensen, E. J. M., Reconstruction of Clean and Oxygen-Covered Pt(110) Surfaces, *J. Phys. Chem. C* **2013**, *117*, 11251-11257.

(15) Fantauzzi, D.; Mueller, J. E.; Sabo, L.; van Duin, A. C.; Jacob, T., Surface Buckling and Subsurface Oxygen: Atomistic Insights into the Surface Oxidation of Pt(111), *ChemPhysChem* **2015**, *16*, 2797–2802.

(16) Holby, E. F.; Greeley, J.; Morgan, D., Thermodynamics and Hysteresis of Oxide Formation and Removal on Platinum (111) Surfaces, *J. Phys. Chem. C* **2012**, *116*, 9942-9946.